

PAPER • OPEN ACCESS

## Study of a diamond channel cut monochromator for high repetition rate operation at the EuXFEL: FEA thermal load simulations and first experimental results

To cite this article: K R Tasca *et al* 2022 *J. Phys.: Conf. Ser.* **2380** 012053

View the [article online](#) for updates and enhancements.

### You may also like

- [Intensity Calibration of Normal Incidence Monochromator by the Double Monochromator Method](#)  
Kozo Ando, Kiyohiko Okazaki and Kazuo Mori
- [Characterization of a versatile reference instrument for traceable fluorescence measurements using different illumination and viewing geometries specified in practical colorimetry—part 1: bidirectional geometry \(45:0\)](#)  
Joanne Zwinkels, William Neil and Mario Noël
- [Monochromator operation in the carbon window region at the reflectometry beamline BL-11D of the Photon Factory](#)  
Tadashi Hatano and Shogaku Aihara

### ECS Toyota Young Investigator Fellowship

For young professionals and scholars pursuing research in batteries, fuel cells and hydrogen, and future sustainable technologies.

At least one \$50,000 fellowship is available annually.  
More than \$1.4 million awarded since 2015!



Application deadline: January 31, 2023



TOYOTA

**Learn more. Apply today!**

# Study of a diamond channel cut monochromator for high repetition rate operation at the EuXFEL: FEA thermal load simulations and first experimental results

K R Tasca<sup>1</sup>, I Petrov<sup>1</sup>, C Deiter<sup>1</sup>, S Martyushov<sup>2</sup>, S Polyakov<sup>2</sup>, A Rodriguez-Fernandez<sup>1</sup>, R Shayduk<sup>1</sup>, H Sinn<sup>1</sup>, S Terentyev<sup>2</sup>, M Vannoni<sup>1</sup>, S Zholudev<sup>2</sup> and L Samoylova<sup>1</sup>

<sup>1</sup> European X-ray Free Electron Laser GmbH, 22986, Schenefeld, Germany

<sup>2</sup> Technological Institute for Superhard and Novel Carbon Materials, Moscow, Russia 108840

E-mail: kelin.tasca@xfel.eu

**Abstract.** The recent start of the European X-ray Free-Electron Laser (EuXFEL) provides a unique pulsed X-ray source of high spectral brilliance and high photon flux at a high repetition rate and opens the possibility for new scientific opportunities. However, the EuXFEL beam has a high peak power that is converted into a high cyclic thermal load on the optical elements, such as mirrors and monochromators, and is impossible to fully mitigate within the pulse train pattern. In the single crystal based X-ray monochromators, the increase of temperature leads to deformation of the crystal structure which affects the rocking curve and consequently the performance of these devices and the quality of the transmitted X-ray beam. To address the increase of temperature, we propose the use of a diamond channel-cut monochromator as an alternative to the current silicon monochromators. In this work we present the design and parameters of the diamond monochromator, heat load simulations and the surface and crystalline quality characterisation. The heat load simulations indicate a high performance of the monochromator under the pulse train of the EuXFEL and the characterisation demonstrates high crystal quality and its functionality as a double crystal monochromator.

## 1. Introduction

The European XFEL (EuXFEL) generates X-ray pulses of femtosecond duration and high pulse energy. Its bunch pattern can deliver up to 2700 pulses within 600  $\mu$ s, which is called the pulse train, at 10 Hz repetition rate [1]. This pulse structure provides high photon fluxes at MHz repetition rate; however, the high peak power is also converted in extreme high thermal load on the optical components, which is impossible to mitigate within the pulse train period, and consequently have their performance reduced.

Currently, in the hard X-ray regime at EuXFEL, cooled double Si(1 1 1) monochromators are used and it was reported a decrease of a factor of 2 in the monochromator transmitted intensity after around 150 pulses [2]. The intensity decrease results from the accumulated heat in the first crystal, which causes variations in the lattice structure and consequently changes in the diffraction profile like broadening of the rocking curve and shift of the central wavelength.



As an alternative to silicon, we propose a diamond channel cut monochromator (DCCM). Diamond has lower X-ray absorption, smaller thermal expansion coefficient and higher thermal conductivity compared to silicon, high reflectivity and narrow rocking curves [3, 4, 5]. Furthermore, advances in HPHT synthesis methods have allowed the growth of large high-quality single crystals type IIa diamond [5, 6]. In this paper, we present the design, the geometrical parameters, energy range of operation, the acceptable temperature drift, heat load simulations and the results of the characterisation by confocal microscopy and rocking curve imaging of the DCCM prototype.

## 2. Monochromator design

The diamond channel-cut monochromator (DCCM), shown in figure 1, was made from a single crystal diamond block of high quality HPHT IIa type diamond of  $4 \times 4 \times 5 \text{ mm}^3$  with  $[1\ 1\ 0]$ ,  $[1\ -1\ 0]$  and  $[0\ 0\ 1]$  crystallographic orientations. The two diffracting surfaces are oriented in the  $[1\ 1\ 0]$  direction, with 2.5 mm length (parallel to the beam direction), 2 mm width, 1 mm thickness and are 2 mm apart. The channel was symmetrically made by laser cutting and the surfaces were not polished.

This design allows the use of reflection  $(2\ 2\ 0)$  or higher orders, depending on the intended energy. As an example of the resulting geometrical and diffracting parameters of the  $C(2\ 2\ 0)$  reflection operating at 9 keV, the beam is vertically offset by 3.3 mm and the theoretical energy resolution is  $1.9\text{E-}5$ .

The dimensions of the monochromator and the beam size pose a geometrical limitation on the energy range of operation. For this channel-cut with a gap of 2 mm and for a beam size of  $100 \mu\text{m}$ , the maximum angular range is from  $24^\circ$  to  $80^\circ$ . In the case of the  $C(2\ 2\ 0)$  reflection, the energy is limited from 5 to 12 keV and for  $C(4\ 4\ 0)$  from 10 to 24 keV. For larger beam sizes, a plot of the energy range as a function of beam size for  $(2\ 2\ 0)$  and  $(4\ 4\ 0)$  reflections is shown in figure 1.

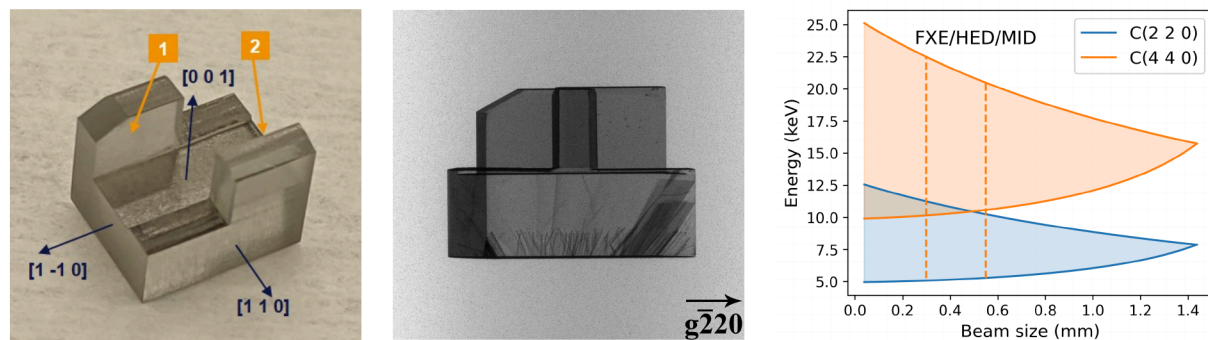


**Figure 1.** The diamond channel-cut monochromator, and its crystallographic orientations (left). The crystal is  $4 \times 4 \times 5 \text{ mm}^3$ . The gap between the diffracting surfaces is 2 mm and was made by laser cutting. The size of each blade is  $2.5 \times 2 \times 1 \text{ mm}^3$  and they are symmetrically oriented. Lang topography taken with  $(\text{AgK}\alpha_1)$  radiation (center). Energy range of operation for  $C(2\ 2\ 0)$  and  $C(4\ 4\ 0)$  reflections as a function of the incident beam size and indication of the typical beam size used at EuXFEL hard x-ray instruments using the Si monochromator (right).

## 3. FEA simulations

In the case of a double-crystal monochromator, the high heat load on the first crystal, which absorbs most of the pulse energy, induces a thermal deformation in the crystal lattice which results in a mismatch of the diffracting planes and a consequent decrease of the transmitted

beam intensity. An acceptable mismatch of the first crystal with respect to the second should be of the same order of Darwin's width, which corresponds to a variation in intensity of a factor of two.

To get an estimate of the temperature change  $\Delta T$  that would lead to this displacement, the coefficient of thermal expansion  $\alpha(T)$  is integrated over the temperature interval  $\Delta T$ , which gives  $\Delta T = 17$  K in the case of  $T_0 = 300$  K and  $\Delta T = 96$  K in the case of  $T_0 = 100$  K.

In order to predict the temperature increase under the thermal load of the EuXFEL beam the heat equation was solved numerically by finite element analysis (FEA) using Comsol Multiphysics. We modelled a 3D diamond crystal with the same dimensions of the DCCM described above under a quasi continuous heat load considering 9 keV X-ray pulses with Gaussian distribution of 0.5 mJ, 0.55 mm at 1.1 MHz and 2.2 MHz repetition rate, corresponding to the same conditions of a typical beam at EuXFEL, with initial temperatures of 100 K and 300 K [2].

The time dependent model considers that the X-ray beam impinges perpendicularly on the first blade and the channel cut is thermally insulated. The effect of the incident angle and of the absorption are taken into account introducing the beam footprint  $b/\sin\theta$  and the effective attenuation length  $l_{att}\sin\theta$  terms in the power density distribution  $Q$ :

$$Q = \frac{4 \ln 2 E_P \left[ 1 - \exp\left(-l/l_{att}\sin\theta\right) \right]}{\pi b^2 l_{att} \tau} \exp\left\{-4 \ln 2 \left[\left(x \sin\theta/b\right)^2 + (y/b)^2\right]\right\} \exp(-z/l_{att}\sin\theta) \quad (1)$$

where  $E_P$  is the pulse energy,  $b$  the beam size,  $\tau$  is the period and  $l_{att}$  the attenuation length.

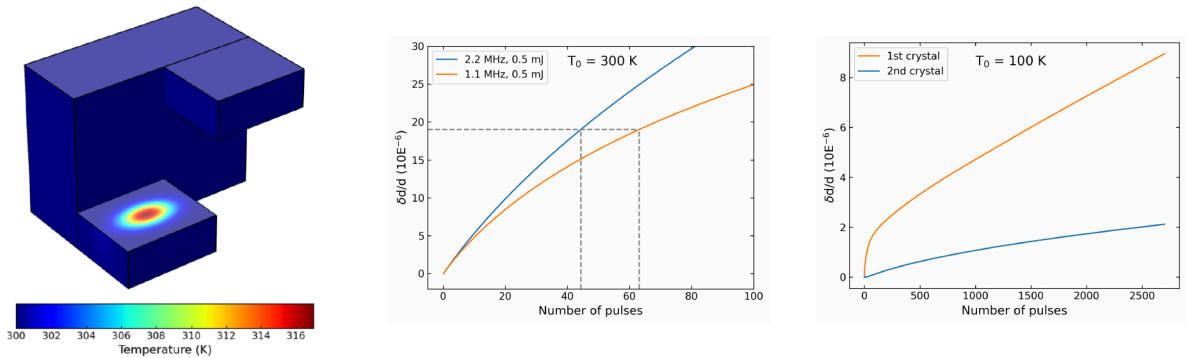


**Figure 2.** DCCM temperature distribution simulation for 9keV pulses of 0.5 mJ, 0.55 mm, and expected lattice parameter variation at room temperature and at 100 K.

At an initial temperature of 300 K, the crystal reaches the acceptable relative lattice parameter variation of  $1.9E-5$  after 65 pulses, for a repetition rate of 1.1 MHz, and after 45 pulses for 2.2 MHz as seen in figure 2.

For the cryogenic case, it was considered a model where the channel cut is fixed to a CVD diamond heat exchanger and the back surface of the heat exchanger is kept at 100 K. The remaining surfaces are thermally insulated. For this initial temperature, the lattice parameter variation, shown in figure 2, is within the acceptable limit for the train of 2700 pulses of the EuXFEL. Here, we also observe that the temperature of the second crystal also increases and thus the misalignment between the two crystals decreases.

#### 4. Crystal characterisation

The surfaces of the two blades of the DCCM were investigated using a confocal microscope NanoFocus  $\mu$ surf custom. The images revealed the presence of almost parallel scratch lines on

the surface of both of the blades as seen in figure 3. These structures have irregular shape and distribution with presence of plateaus. An estimated analysis of the profile shows local distances peak to valley from 0.6 to 10  $\mu\text{m}$ , width of 5 - 13  $\mu\text{m}$  and plateau width of  $\sim 20 \mu\text{m}$  in both crystals.

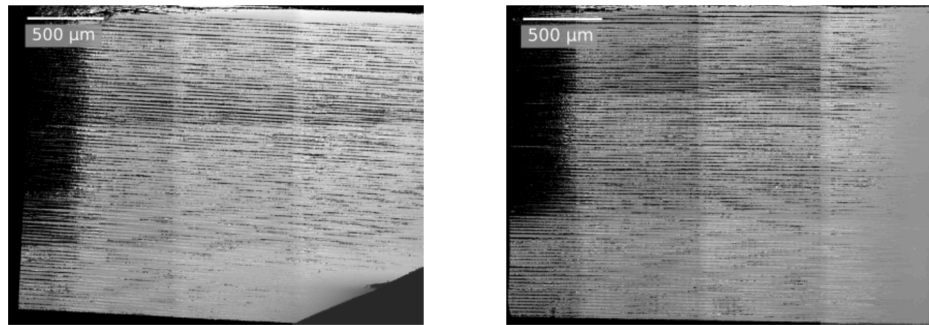


**Figure 3.** Confocal microscopy images of the two blades.

The lines result from the laser cutting process. In the cutting process the incident 532 nm pulsed laser beam (100 ns) has a spot size of 20-25  $\mu\text{m}$  and hits the sample at an angle of  $3^\circ$  moving along the surface in steps of 6  $\mu\text{m}$ .

The crystal quality of each individual blade was investigated by rocking curve imaging (RCI) [7]. In the RCI method the diffracted signal of each point of the rocking curve is recorded by a 2D detector. It thus combines the advantages of topography and diffraction profile analysis and in this way it is possible to generate maps of the width, peak position and intensity of the rocking curves.

The RCI measurement was performed at PETRA III beamline P23 with photon energy of 18 keV, a Si(1 1 1) monochromator and the beam was focused to a size of  $50 \times 100 \mu\text{m}^2$ , in vertical and horizontal directions. The crystal was aligned to diffract the C(2 2 0) planes at the Bragg angle  $15.85^\circ$ , which enables each blade to be studied individually. In order to probe the entire surface, the crystal was translated in steps of 0.3 mm in the direction parallel to the beam, and in steps of 0.15 mm perpendicularly to the beam direction. For each sample position the crystal was rotated around its diffraction angle, performing an omega scan to measure the rocking curve. At each point of the rocking curve a topography was recorded by an area detector with  $55 \mu\text{m} \times 55 \mu\text{m}$  pixel size positioned perpendicular to the diffracted beam. The rocking curves were reconstructed integrating the intensity in a detector area of  $220 \times 275 \mu\text{m}^2$ .

The curves were fitted to a Gaussian function to determine the rocking curve full width at half maximum (FWHM), peak position and intensity. The rocking curves of each blade, measured at the center of the blades and the curve fitting, are shown in figure 4. The FWHM of the both blades are  $5.8''$  and  $5.9''$ . These widths are broader than the intrinsic width of the C(2 2 0) reflection of  $1.1''$  predicted by the dynamical theory of X-ray diffraction [8, 9]. However, due to the mismatched angles between Si(1 1 1) and C(2 2 0) and to the divergence of the incident beam it is expected the broadening of the diffraction profile.

The fitted FWHM, that indicates the crystal quality, of the entire surface of each blade are represented in the RCI maps shown in figure 5.

With the exception of individual regions near the edges of the crystal, the maps of FWHM demonstrate a variation of the rocking curve width from  $5.6''$  to  $6''$  in the first crystal and from  $5.6''$  to  $8''$  in the second crystal. Furthermore, we can see that the distribution of the FWHM is uniform, within the limits of the experimental setup, and indicates a good crystal quality.

To verify the exit beam from the DCCM after two successive reflections, we rotated the crystal

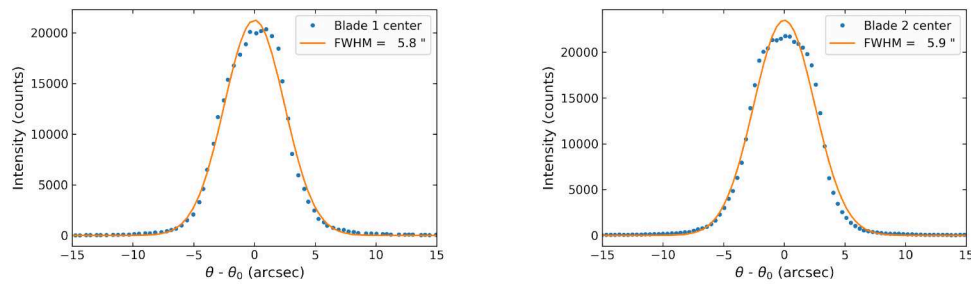


**Figure 4.** Rocking curves of each blade.

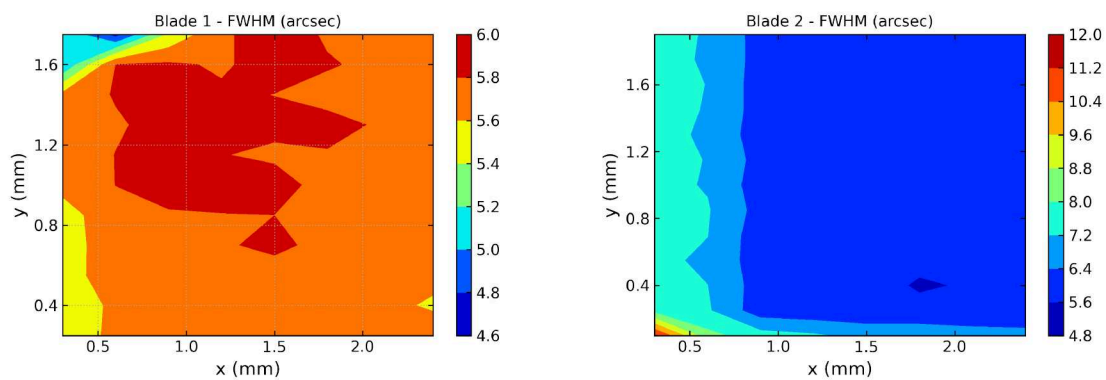


**Figure 5.** Maps of the FWHM of each blade of the DCCM.

to  $33.1^\circ$  to change the reflection to  $C(4\ 4\ 0)$  at 18 keV and the same procedure as described above was done. On the left of figure 6, it shows in blue, the measured diffraction profile of the double-bounce reflection  $C(4\ 4\ 0)$  at the center of the DCCM, the orange line is the  $C(4\ 4\ 0)$  Darwin curve and the green line is the  $Si(1\ 1\ 1)$  theoretical bandwidth. On the right it is shown a map of the FWHM.

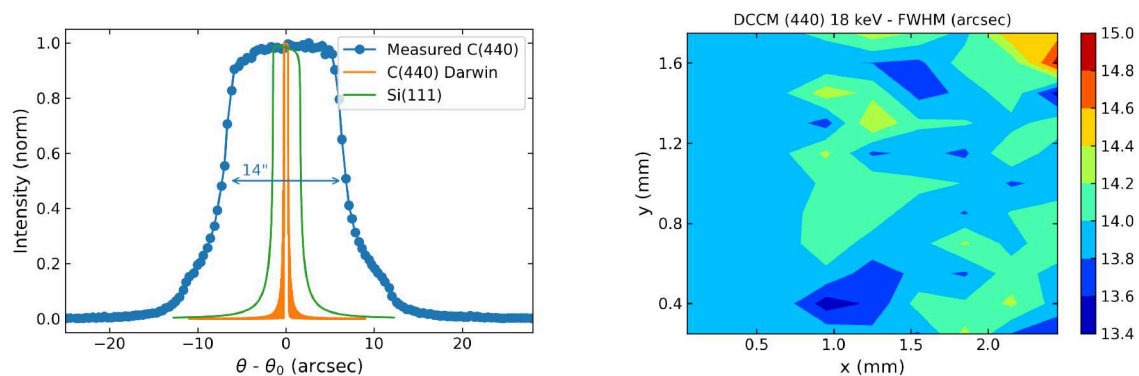


**Figure 6.** Left: Double bounce reflection profile from the DCCM  $(4\ 4\ 0)$ ,  $C(4\ 0\ 0)$  Darwin curve and  $Si(1\ 1\ 1)$  bandwidth. Right: Distribution map of the measured width (right).



## 5. Conclusions and Outlook

We presented the design and parameters of a diamond channel cut monochromator that could be an alternative to the current Si monochromator used in EuXFEL. The channel cut design ensures high mechanical stability while diamond has higher thermal conductivity and resilience to high thermal loads. The DCCM was designed to operate in an energy range of 5 - 25 keV, depending on the beam size, and could be suitable for FXE, MID and HED instruments of the EuXFEL. The FEA simulations predict a high efficiency of the beam transmission at high heat loads. At 300 K without cooling is expected a transmission of up to 65 pulses with a decrease of 50% of the intensity. At 100 K high transmission (>50%) is predicted within the entire pulse train. These estimates should be confirmed with a proof of principle experiment at EuXFEL foreseen. The metrology characterisation showed some features in the surface, which can be improved with the polishing and the X-ray measurements demonstrated the high crystal quality and the functionality of the DCCM as a monochromator.

## Acknowledgments

This work is supported by the R&D program of EuXFEL, Schenefeld, Germany. We acknowledge DESY (Hamburg, Germany), a member of the Helmholtz Association HGF, for the provision of experimental facilities and computational infrastructure. Parts of this research were carried out at PETRA III and we would like to thank D. Novikov and Y. Matveev for assistance in using beamline P23 and through Maxwell Cluster computing platform.

## References

- [1] W Decking *et al* 2020 A MHz-repetition-rate hard X-ray free-electron laser driven by a superconducting linear accelerator *Nat. Photonics* **14** 391-397
- [2] I Petrov, U Boesenberg, V A Bushuev, J Hallmann, K Kazarian, W Lu, J Möller, M Reiser, A Rodriguez-Fernandez, L Samoylova, M Scholz, H Sinn, A Zozulya and A Madsen 2022 Performance of a cryo-cooled crystal monochromator illuminated by hard X-rays with MHz repetition rate at the European X-ray Free-Electron Laser *Opt. Express*. **30** 4978-87 10.1364/OE.451110
- [3] C Giles, C Adriano, A Freire Lubambo, C Cusatis, I Mazzaro and M G Hönnicke 2004 Diamond thermal expansion measurement using transmitted X-ray back-diffraction *J. Synchrotron Radiat.* **12** 349-353
- [4] A V Inyushkin, A N Taldenkov, V G Ralchenko, A P Bolshakov, A V Koliadin, and A N Katrusha 2018 Thermal conductivity of high purity synthetic single crystal diamonds *Phys. Rev. B* **97**, 144305
- [5] R C Burns, A I Chumakov, S H Connell, D Dube, H P Godfried, J O Hansen, J Härtwig, J Hoszowska, F Masiello, L Mkhonza, M Rebak, A Rommevaux, R Setshedi and P Van Vaerenbergh 2009 HPHT growth and x-ray characterization of high-quality type IIa diamond *J. Phys.: Condens. Matter* **21** 364224
- [6] S N Polyakov, V N Denisov, N V Kuzmin, M S Kuznetsov, S Yu Martyushov, S A Nosukhin, S A Terentiev and V D Blank 2011 Characterization of top-quality type IIa synthetic diamonds for new X-ray optics *Diamond and Related Materials* **20** 726-728
- [7] D Lübbert, T Baumbach, J Härtwig, E Boller and E Pernot 2000  $\mu$ m-resolved high resolution X-ray diffraction imaging for semiconductor quality control *Nucl. Instrum. Methods Phys. Res. B* **160** 521-27
- [8] A Authier 2003 *Dynamical Theory of X-Ray Diffraction* (Oxford: Oxford University Press)
- [9] M S del Rio and R J Dejus 2011 XOP v2.4: recent developments of the x-ray optics software toolkit *Adv. Comput. Methods X-Ray Opt. II* **8141** 368-372